RSC Advances

ROYAL SOCIETY OF CHEMISTRY

www.rsc.org/advances

Temperature and thickness dependence of the sensitivity of nitrogen dioxide graphene gas sensors modified by the atomic layer deposited Zinc Oxide films

Haifen Xie[a], Keke Wang[a], Zhiqiang Zhang[a], Xiaojing Zhao[b], Feng Liu[b], Haichuan Mu[a] *

a. Department of Physics, School of Science, East China University of Science and Technology, 130 Meilong Road, Shanghai 200237, Shanghai, China

b. Department of Physics, Shanghai Normal University, 100 Guilin Road, Shanghai 200234, Shanghai , China

Abstract

The Chemical Vapor Deposition (CVD) grown graphene nitrogen dioxide (NO_2) gas sensors modified by the Zinc Oxide (ZnO) thin films via atomic layer deposition (ALD) were fabricated and their sensitivity dependence on the temperature and ZnO films thickness was investigated. The anomalous p-type response of the ALD ZnO modified graphene sensors (ZnO/graphene) to NO_2 at room temperature was found which might be attributed to the n to p conductance transition due to the reaction between oxygen vacancies and oxygen in the ZnO films. At elevated temperature, ZnO/graphene sensors exhibited p to n conductance transition and the transition temperature increased from 200°C for pristine graphene, 300°C for 5 ALD cycles and 1nm ZnO/graphene, to 350°C for 3, 5 and 10nm ZnO/graphene. Meanwhile, the sensors sensitivity revealed strong temperature dependence with the optimal temperature of 100°C for ultra thin 5 ALD cycles ZnO/graphene (including pristine graphene) and 200°C for other ZnO/graphene sensors (ZnO films thickness ≥ 1nm). Such transition and sensitivity dependence on temperature could be ascribed to the change of carriers type and concentration in the ZnO/graphene with the variation of the temperature. Besides, Strong sensitivity dependence on the ZnO films thickness at various temperatures was also demonstrated with the optimal ZnO films thicknesses

of 5 ALD cycles for relatively low temperature of 100°C and 3nm for higher temperature of 200°C and 300°C. The mechanism responsible for the sensors sensitivity dependence on the temperature and ZnO films thickness was discussed.

Key words: graphene, zinc oxide (ZnO), Atomic Layer Deposition (ALD), temperature and thickness dependence, sensitivity,

1. Introduction

The accurate and prompt detection of the hazardous and oxidizing nitrogen dioxide (NO_2) gas is of great importance for the environmental protection. Graphene as a widely recognized promising new material has been extensively investigated as chemical sensors[1-6] because of its specific characteristics, such as high surface to volume ratio, high conductivity, low Johnson noise and less defects for low 1/f noise[,5,7-11]. Among all kinds of graphene fabrication methods, Chemical Vapor Deposition (CVD) [7-8,12-16] stood out because of its capability to make large area and high quality graphene films in mass production scale compared to others like exfoliated graphene[8] and reduced graphene oxide[17]. Besides, the monolayer graphene sensors were demonstrated to show better gas sensitivity compared to that of the multilayer ones because of the higher surface to volume ratio together with the interlayer coupling effect resulted from the additional parallel conduction path (graphene layers) for the multilayer ones[1]. However, it was difficult for the sole graphene gas sensors to reach the detection limit down to parts-per-billion (ppb) level because of the relatively weak adsorption/reactions of the target gas molecules with the graphene surface[1,8]. Meanwhile, typical metal oxide semiconductors like Zinc Oxide (ZnO), Tin Dioxide (SnO_2) and Indium Trioxide (In_2O_3) were widely recognized as excellent semiconductor gas sensing materials in detecting hazardous or flammable gases like nitrogen dioxide (NO_2), carbon oxide (CO) and hydrogen (H_2)[18]. In addition to those traditional bulk sized metal oxides semiconductor materials, various nanoscale forms of metal oxides were also developed to further improve the sensitivity and selectivity to hazardous/flammable gases. Wang et.al[19] introduced high sensitivity ZnO nanotube gas sensors exhibiting sensitive response to NO_2 down to 500 ppb at 30°C. ZnO quantum dots were also fabricated at room temperature with

good sensitivity to 2 parts-per-million (ppm) NO_2 at 200°C[20]. Zhang et.al[21-22] reported the high selectivity and sensitivity of the SnO_2 and ZnO hollow-sphere sensor for NO_2 sensing and demonstrated the strong dependence of the sensors sensitivity on the crystallite size. Besides, nano-sized metal oxides gas sensors added with various dopants also demonstrated improved sensitivity and selectivity, like p-and n-type Fe-doped SnO_2[23] and polyvinylpyrrolidone-modified ZnO nanopartcles[24]. Moreover, the combination of the nanoscale metal oxides with graphene oxides derived graphene for superior gas sensitivity was also reported, for example, 3D array structures containing highly aligned SnO_2 nanorods on graphene sheets exhibited high H_2S gas sensitivity, and such enhanced performance resulted from the large surface area of SnO_2 nanorods array and the superior electronic characteristics of graphene [25]. Zhang et.al also reported SnO_2 nanoparticles-reduced graphene oxide nanocomposites for NO_2 sensing[26]. Therefore, improved sensors performance based on the hybrid effect of the graphene and nanoscale metal oxides semiconductors could be possibly achieved because of the high surface to volume ratio of the graphene and strong reactivities of the metal oxides[27]. However, it was noteworthy that almost all above mentioned nanoscale metal oxides sensors were prepared by time-consuming and tedious wet chemical procedure, which not only complicated the fabrication processing and possibly introduced the impurities into the sensors but also was not compatible with the CVD grown graphene films. Such rough wet chemical procedure would cause severe damage to the CVD grown graphene and deteriorate its electrical property, thus obstructed the improvement of the sensitivity. Atomic layer deposition (ALD), on the other hand, was famous for its unique characteristics of obtaining uniform and conformal films at atomic precise level without serious damage to the substrate due to its low temperature and chemisorptions process. So, the ALD processing would fulfill

the metal oxides films deposition without the damage to the graphene and avoid any deterioration of its electrical properties. In this paper, ZnO films with various thicknesses were fabricated by atomic layer deposition (ALD) on CVD grown monolayer graphene films. The sensitivity dependence of the ALD ZnO/graphene sensor on the temperature and ZnO films thickness as well as the corresponding sensing mechanism was discussed.

2. Experimental

Graphene films with the size of 2cm × 2cm were fabricated via typical Low Pressure Chemical Vapor Deposition (LPCVD) at the temperature of 1035°C and the total working pressure of 100 Pa. A routine procedure was performed with the 30 minutes annealing of Copper (Cu) foils in H_2 prior to the 1 hour graphene growth at the mixture of CH_4 and H_2 with the flow ratio of 1:10 standard-state cubic centimeter per minute (sccm) (2:20 sccm). Spin-coated poly-methylmethacrylate (PMMA) layer was employed to transfer the graphene films to SiO_2(300nm)/Si wafers, and the underlying Cu foils was dissolved by iron nitride solution. The transferred grpahene films were further annealed at 375°C in the atmosphere of Ar and H_2 (150sccm:50sccm) for 90 minutes to get rid of all PMMA residues. Afterwards, the ALD was employed to deposite ZnO films on annealed graphene films (Cambridge Naonotech ALD 100 system), in which diethylzinc (DEZ, $Zn(C_2H_5)_2$)(Aldrich) and deionizer water (H_2O) was applied as Zn and O precursor, respectively, with the growth temperature of 80°C and the operating pressure of 8×10^{-3}Pa. In the ZnO ALD processing, precursors and purge gases were alternately introduced into the growth chamber with the cycle of DEZ/N_2/H_2O/N_2 and the respective exposure time of 15ms/20s/15ms/20s, where N_2 gas (99.9999%) was used as carrier and purge gas. The calibrated thickness of the 1000, 3000 and 5000 cycles ALD ZnO films on the

graphene were 100nm, 300nm and 500nm, which led to the ZnO films thickness of 1nm, 3nm, 5nm, and 10 nm through the adjustment of the corresponding ALD cycles number to 10, 30, 50 and 100, respectively. It was noteworthy that the impact from the roughness of the base graphene films would be overwhelming while the thickness of the ZnO film was below 1nm (ALD cycles was less than 10), and derived ZnO films thickness based on ALD cycles might not be accurate in that case due to the discontinuous nature of the ultra thin ZnO films, therefore for the ZnO films fabricated via 5 ALD cycles, the thickness was represented by 5 cycles instead of the 0.5nm.

For gas sensing test, silver (Ag) paste was drop coated on the edges of the ZnO modified graphene films acting as electrodes and the contacting pads connecting to the sensitivity test equipment (Gimix, USB/RS485 1.5) were directly pressed on the Ag electrodes. A self-made stainless jar with the gas inlet and outlet as well as the testing samples holder equipped with the heater for temperature variation was employed as gas chamber for sensors sensitivity test. During the test, the fabricated sensors were placed on the sample holder with the temperature varied from 25°C to 350°C at the relatively humidity (RH) level of 50% in a 1000 class clean room. Usually, the sensors were exposed to dry air flow (500 sccm) for 40 minutes to achieve stable initial resistance (R_o) at various temperatures. Then the mixture of dry air and NO_2 with different flow rate ratio, which resulted in different concentration of NO_2 ranging from 10 ppm to 200 ppb, was introduced into the testing chamber and lasted for 10 minutes with the constant flow rate of 500 sccm. The compressed dry air was injected into the chamber for 20 minutes subsequently for recovery. The ratio of $(R_g-R_o)/R_o$, where R_g stood for the sensors resistance upon exposure to NO_2 , was defined as the sensors response.

Besides, all graphene films were subjected to ozone treatment prior to the ALD processing to break the chemical inertness of the as-grown graphene[28-29]. It was noteworthy that the as-grown graphene surface was not suitable for deposition of any films by ALD because of its chemical inertness and the functionalization of the graphene films prior to the ALD processing was necessary. The pristine graphene films in the study represented the as-grown graphene after ozone treatment, and such functionalization was performed by 254nm Ultraviolet (UV) lamp for 90 seconds at the power of 20mw/cm^2. Field Emission Scanning Electron Microscope (FESEM) and Raman Spectrum were employed to characterize the ZnO/Graphene films surfaces morphology and structures, respectively, while X-ray Photoelectron Spectroscopy (XPS) was applied to check the films bonding states.

3. Results and discussion

3.1 Morphology and structure of the ALD ZnO films on graphene

Surface morphology of the pristine graphene on SiO_2/Si substrates after 375°C annealing was shown in Fig.1(a). Apparently, PMMA residues could still be observed and resulted in remarkably higher roughness of about 2.5 nm compared to that of exfoliated graphene (0.1nm)[28] (AFM images, not shown here). PMMA leftovers could be further demonstrated by the high magnification FESEM image (Fig.1(a) inset). Fig.1(b) indicated the surface image of the 5 cycles ZnO modified graphene, which clearly revealed the discontinuous ZnO film with some parts of the base graphene uncoated. Such unique surface morphology could be the results of the ultra thin ZnO films thickness and high graphene surface roughness above mentioned. The PMMA remaining showed much smaller size due to the partly coverage by ZnO as indicated by the high magnification picture (Fig.1(b) inset). After 3nm and 10nm ZnO deposited by ALD on graphene, continuous and compact films were observed as

shown in Fig.1(c) and (d), which demonstrated that the graphene surface was coated by ZnO films. Moreover, there were grain boundaries existing in the ZnO films, which resulted from the grain boundaries in the base graphene film inherited from the annealed copper foil. Under high magnification, the grain boundaries in the thicker 10nm ZnO was apparently much spectacular compared to those of other ZnO films.

To further demonstrate the existence of the ZnO films, XPS spectra was employed to characterized the ZnO/graphene films, and the existing Zn-O bond was clearly demonstrated as well as the remarkable difference in oxidation for 5 cycles and 10nm ZnO films. Fig.2(a) and (b) showed the Zn2p and O1s scan of the 5 cycles and 10nm ZnO/graphene films, respectively. For the 5 cycles ZnO/graphene, the intensities of the Zn2p3 and Zn2p1 lines were much weaker compared to those of 10nm ZnO modified one together with a larger noise level, which demonstrated its thin ZnO films thickness (see Fig.2(a)). Furthermore, the difference in the ZnO films thickness could also be apparently distinguished by the different extent of the oxidation as shown in Fig.2(b). The O1s peak could be deconvoluted into couple components, and within them, Zn-O bond with the binding energy around 530.8ev was clearly observed for both thicknesses. Carboxylic (533.7ev for O-C=o, 531.4ev for o-C=O, capitalized O represented the oxygen bonding state) was clearly observed for 10nm ZnO/graphene compared to that of 5 cycles ZnO modified one besides the dominant ethers (532.7ev) and Zn-O bond for both thicknesses, which proved more serious oxidation occurred in the case of 10nm ZnO ALD processing.

Fig.3 showed the Raman spectra of the as-grown, pristine (after 90s ozone treatment), and 5 cycles and 10nm ZnO/graphene films. The monolayer graphene with no detectable defects (D peak) was clearly demonstrated for as grown graphene as well as the appearance of the defects (D peak) for the pristine (ozone treated) one

with the calculated G/D peak intensity ratio of 3.3. After the 5 cycles and 10nm ZnO films modification, the G/D peak intensities would further decreased to 3.1 and 2.7, respectively, which proved the deterioration of the graphene structure, and coincided well with the more serious oxidation for 10nm ZnO/graphene demonstrated by the previous XPS spectra.

3.2. Temperature dependence of the NO_2 sensitivity

In our study, all the sensors revealed p-type response behavior upon the exposure to NO_2 (showing the decreasing of the resistance) at room temperature. Most of metal oxide semiconductors, such as ZnO, SnO, WO_3 and Fe_2O_3 were usually considered as n-type semiconductor[18], which showed the resistance decrease upon the exposure to reducing gas like H_2, CO and vice versa to oxidizing gas like NO_2, O_2. Although the sensing mechanism of the metal oxides gas sensors was still controversial and not fully understood, a sensing mechanism involving two aspects was well accepted[18]: electronic change of the oxide surface through the target gas-solid interaction and the transduction of the surface phenomenon into an electrical resistance change of the sensor. Oxygen adsorbates like O_2^-, O^- and O_2^- were generated by adsorbed oxygen extracting electrons from the oxides conduction band and resulting in the electron depletion layer on the surface. The surface reactions between the target gas molecules and oxygen adsorbates would lead to a change in the electron depletion layer and finally the sensors resistance. In normal case of detecting NO_2, the resistance of the sensor could be modulated by the reaction between the NO_2 and oxygen adsorbates. NO_2 was a strong oxidizing gas, and it would accept electrons through the surface reactions and increased the width of the electron depletion layer. Thus, the resistance of the n-type metal oxides sensor would be raised. However, there were lots of reports regarding the anomalous n to p conductance transition of

typical n-type metal oxide semiconductors, which could be found in various oxides, like In_2O_3[30], SnO_2[23], MoO_3[31]. Furthermore, the mechanism responsible for this anomalous transition was still uncertain, and various explanations was proposed such as the results of surface reaction[23,30] and oxygen adsorption[32]. It was noteworthy that the study on the metal oxide semiconductor conduction transition was of great importance to control the sensors selectivity, and would be beneficial for the thorough understanding of the metal oxides semiconductor sensing mechanism. In our case, oxygen vacancies might exist in a possible metastable state, whose formation could be represented by the following reaction[33]: $O_o^* \leftrightarrow 1/2\ O_2(g)+V_o^{2+}+2e^-$, where O_o^* represented an unstable oxygen atom in an oxygen site, and V_o^{2+} an oxygen vacancy with double positive charge. Such unstable oxygen atom might result from the specific low temperature of 80°C employed in our ALD processing to avoid serious damage to the basic graphene films. During the oxygen adsorption, oxygen was incorporated into the vacancies, corresponding reaction could be shown as: $[V_o^{2+}] +1/2\ O_2 \leftrightarrow O_o+2h^+$, where O_o and h^+ stood for the oxygen atom in an oxygen site and single charged hole, respectively[31,33]. Meanwhile, the oxygen adsorption on the bare graphene would lead to the charge transfer, in which the oxygen acted as electron acceptor and made the graphene show p-type conductance[34]. In case the generated holes concentration from the oxygen incorporation in the ZnO and p-type doped graphene was larger than the intrinsic electron concentration, n to p conductance transition occurred for ZnO/graphene sensors. With the increasing of the operating temperature, all sensors exhibited the improved sensitivity as shown in Fig.4(a)-(f) and Table 1. Apparently, the pristine graphene demonstrated the minimum improvement compared to that of room temperature (from 4.4 to 8.2%) while ZnO modified graphene sensors showed much remarkable enhancement of the sensitivity.

Such difference could be attributed to the absence of ZnO films, which diminish the reaction between NO_2 and oxygen adsorbates. For pristine graphene, the sensing mechanism could be interpreted as to the change of interface charge layer by the adsorption and reaction of oxygen and target gas molecules[8,35], so the sensitivity was controlled by the factors causing the variation of interface charge layer including oxygen adsorption/desorption and the reaction between NO_2 and oxygen adsorbate. During such reaction, the NO_2 would accept electrons and therefore enhanced the p-type conductance[19,21]. At elevated temperature, the transition of the conductance type would be controlled by the competition between the desorption of the oxygen adsorbates and reactions between adsorbates and NO_2. The former one led to the decrease of the p-type conductance while the later one increased it. The two opposite effects reached the balance at certain temperature of 200°C and conductance transition happened. The slight improvement of the sensitivity at 100°C could be ascribed to the more intense reaction at elevated temperature. With the further increasing of the operating temperature exceeding 200°C, the desorption apparently dominated the sensitivity behavior and the influence from the surface reaction became weaker because more oxygen adsorbates desorbed, which resulted in the similar response behavior at 200 °C and 300°C for pristine graphene.

For ZnO modified graphene, the graphene would mainly act as a NO_2 sensor because of its high surface to volume ratio, so the superior performance compared to pristine graphene resulted from the combining effect of sensitive graphene base as well as active ZnO reaction centers. Moreover, the increasing of the operating temperature would cause not only the enhanced desorption of oxygen adsorbates but also dramatic thermal excitation of the electrons in the ZnO valence band to conduction band[36], both of which led to the increasing of the electron concentration of

ZnO. However, the oxidizing gas NO_2 would react with the oxygen adsorbates and accepted electrons, which actually decreased the electron concentration of ZnO[19,21]. Therefore, the sensitivity performance of the ZnO modified graphene sensors at elevated temperature would be the summing effect of the oxygen desorption, thermal excitation and surface reaction between the oxygen adsorbates and NO_2. The increasing of the operating temperature would lead to the enhancement of oxygen desorption, thermal excitation and surface reaction rate of adsorbate with NO_2, two former of which resulted in the increase of the electron concentration (decrease of hole concentration) while vice versa for the last one. Those factors reached the balance at certain temperature for the certain thickness of ZnO/graphene sensors, which reflected the point of p to n conductance transition. With the further increasing of the operating temperature, thermal excitation became dominant because the surface reaction was limited by the enhanced desorption of the oxygen adsorbates although the surface reaction rate was increased, which would favor the n type conductance and simultaneously lower the sensitivity. At high temperature of 350°C, the sensitivity was almost negligible compared to those at lower temperature because of the serious desorption of the oxygen adsorbates (see Table 1).

It was noteworthy that the p to n transition temperature rose from 200°C for pristine graphene to 300°C for 5 cycles and 1nm ZnO/graphene, and even further increased to 350°C for 3nm, 5nm and 10nm ZnO/graphene. Apparently, the transition point rose up with increasing of the operating temperature, and saturated after the ZnO thickness reaching 3 nm. With the modification of the thin layer of ZnO films (5 cycles and 1nm), NO_2 and oxygen species adsorption together with the reaction of oxygen adsorbates with NO_2 was enhanced compared to pristine graphene because the thin and discontinuous ZnO films led to higher surface to volume ratio (see Fig.1(b)).

Such enhancement would raise the holes concentration, and therefore more compensation electrons required to make the p to n transition happen, which resulted in higher transition temperature because the electron thermal excitation of the semiconductor was directly related to the temperature[36]. For the case of thicker ZnO films (3, 5 and 10nm), the Debye length played the dominant role in the sensitivity performance. The Debye length of the semiconductor was directly related to the temperature and carriers concentration[37]. And there were reports of 3-5nm Debye length of the ZnO and SnO_2 films at the temperature of 250-300°C[38-39], which was also corresponding to the maximum sensitivity response. When the ZnO films thickness was close or equal to Debye length, the whole film was in the space charge region and the surface reaction of oxygen adsorbates with NO_2 would be capable to modulate the charge conduction of the entire films, which required higher temperature to generate more electrons to make the compensation and fulfilled the p to n transition. With the further increasing of the ZnO films thickness to 5 and 10nm, which exceeded the Debye length, large part of the films thickness wouldn't be influenced by the surface reaction. Therefore the influence on the carriers concentration from the surface reaction would be saturated and resulted in the stabilized p to n transition temperature.

Moreover, all the pristine and ZnO modified graphene sensors showed the similar volcano shape temperature dependence and coincided well with the model for the oxide semiconductors[18] (see Fig.5(a)). Volcano shape temperature dependence of the oxide semiconductor gas sensor were widely reported and such behavior was attributed to the competition between the enhanced surface reaction and decreasing target gas penetrating depth with increasing of the operating temperature. The

temperature corresponding to the maximum response represented the point at which above two opposite effects reached the balance.

3.3 Thickness dependence of the NO_2 sensitivity

Strong sensitivity dependence on the ZnO films thickness at various temperature was also observed (see Fig.5(a)). At room temperature and relatively low temperature of 100°C, the ZnO modified graphene sensors sensitivity showed the optimal response at 5 cycles and decreased with the increasing of the ZnO films thickness, which indicated that the thin and porous films would be more beneficial for the target gas NO_2 diffusion, oxygen adsorption and therefore lead to more surface reactions although the surface reaction rate was relatively small due to the low operating temperature[18,40]. With the increasing of the ZnO films thickness, the target gas penetrating depth was greatly reduced and resulted in the decreasing sensitivity. Such performance was quite different from those at higher temperature of 200°C and 300°C, in which the 3nm ZnO modified graphene showed the largest response. The interpretation for that difference was the different role of ZnO Debye length at various temperatures. At room temperature and relatively lower temperature of 100°C, oxygen adsorption, target gas NO_2 diffusion and surface reaction was dominant because of the relatively weak oxygen desorption, which made the ZnO films structure and morphology played the decisive role. However, oxygen desorption and thermal excitation took over and became the major effect in determining the ZnO/graphene sensors performance at higher temperature, and brought the ZnO Debye length be the vital factor in sensors performance. The oxygen desorption and thermal excitation would increase the electron concentration (decrease the hole concentration), and therefore dramatically decrease the number of the free carriers in the p-type ZnO. Such reduced free carrier concentration would be more sensitive to

the charge conduction change resulted from surface reaction when the ZnO films thickness was close or equal to Debye length. As mentioned before, the surface reaction could influence the charge conduction of the whole ZnO films at Debye length due to the extension of space charge region inside the entire films. Therefore, the entire covering of the space charge region together with the small concentration of the free carriers made the ZnO/graphene films reached the optimal sensitivity. With the further increasing of the ZnO films thickness to 5 and 10nm, which would exceed the Debye length, large part of the films thickness would not be influenced by the surface reaction, therefore sensors sensitivity deteriorated. Fig.5(b) revealed the sensitivity dependence on the NO_2 concentration for the 3nm ALD ZnO/graphene sensors at the operating temperature of 200°C. A remarkable response of 38% at 10ppm with the detection limit down to 200ppb could be observed.

4. Conclusions

The ALD ZnO/graphene NO_2 gas sensors with various thickness of ZnO films were fabricated and their sensitivity dependence on temperature and thickness were investigated. All ALD ZnO/graphene sensors showed anomalous p-type sensing behavior due to the reaction of oxygen vacancies with oxygen in the ZnO films. Besides the routine volcano-shaped temperature dependence of the sensitivity, which revealed the optimal temperature of 100°C for ultra thin 5 cycles ZnO/graphene (including pristine graphene) and 200°C for other ZnO/graphene sensors (ZnO films thickness ≥ 1nm), the strong temperature dependence of the p to n conductance transition of the ALD ZnO/graphene was observed. Such dependence could be ascribed to the combining effect of the oxygen desorption, thermal excitation and surface reaction between the oxygen adsorbates and NO_2, two former of which resulted in the increase of the electron concentration (decrease of the holes

concentration) while vice versa for the last one. The balance point represented the temperature for p to n conductance transition, above which, the enhanced desorption of the oxygen adsorbates would obstruct the surface reaction and deteriorate the sensitivity. The transition temperature rose up from 200°C (pristine graphene), 300°C (5 cycles and 1nm ZnO/graphe) to 350°C (3, 5 and 10nm ZnO/graphene), and such temperature dependence resulted from the increasing of the electron compensation required to fulfill the conductance transition because of the rising holes concentration. The increasing of the holes concentration was generated from the enhanced adsorption and surface reaction of oxygen and NO_2 at the thin and porous ZnO films surface, and the thorough charge modulation from the Debye length for thicker ZnO films. With further ZnO films thickness exceeding Debye length, the influence on the carriers concentration from the surface reaction would saturate and result in the stabilized transition temperature. Strong sensitivity dependence on the ZnO films thickness at various temperatures was also demonstrated with the optimal ZnO films thicknesses of 5 cycles for relatively low temperature of 100°C and 3nm for higher temperature of 200°C and 300°C. Such difference revealed that oxygen adsorption, target gas NO_2 diffusion and surface reaction, namely the ZnO films surface morphology, was dominant at relatively low temperature while the Debye length of ZnO became the vital factor for sensitivity at higher temperature. Reduced free carrier concentration, which was generated by the enhanced oxygen desorption and thermal excitation in the p-type ZnO at higher temperature, would be more sensitive to the charge conduction change resulted from surface reaction when the ZnO films thickness was close or equal to Debye length. The entire covering of the space charge region at Debye length together with the small concentration of the free carriers at higher temperature made the ZnO/graphene films reached the optimal sensitivity. The

optimal sensors performance with the response of 38% at the 10ppm NO_2 concentration and the detection limit of 200ppb was obtained for the 3nm ALD ZnO/graphene sensors at 200°C.

References

1.R.Pearce, T.Lakimov, M.Andersson, L.Hultman, A.Lloyd Spetz, R.Yakimova, *Sens.Actuators.B*., 2011, **155**, 451-455

2.S.V.Samsonau, S.D.Shvarkov, F.Meinerzhagen, A.D.Wieck, A.M.Zaitsev, *Sens.Acutaturs B.,* 2013, **182**, 66-70

3.F.Yavari, E.Castillo, H.Gullapalli, P.M.Ajayan, and N.Koratkar, *Appl.Phys.Lett.*, 2012, **100**, 203120

4.M.G.Chung, D.H.Kim, H.M.Lee, T.Kim, J.H.Choi, D.K.Seo, J.-B.Yoo, S.-H.Hong, T.J.Kang and Y.H.Kim, *Sens.Actuators B*., 2012, **166**, 172-176

5.H.J.Yoon, D.H.Jun, J.H.Yang, Z.Zhou, S.S.Yang, M.M.-C.Cheng, *Sens.Acutators B.,* 2011,**157**,310-313

6.A.Huang, D.Zeng, H.Li, C.Xie, *Nanoscale,* 2012, **4**, 5651-5658

7. A. K.Geim, K. S.Novoselov, *Nat. Mater*., 2007, **6**, 183-191

8.F.Schedin, A.K.Geim, S.V.Morozov, D.W.Hill, P.Blake, M.I.Katsnelson, K.S.Novosetov, *Nat.Mater.,* 2007, **6**, 652-655

9.X.Du, I.Skachko, A.Barker, E.Y.Andrei, *Nat.Nano.,* 2008, **3**, 491-495

10.K.S.Novosetov, A.K.Geim, S.v.Morozov, D.Jiang, M.L.Katsnelson, I.N.Grigorieva, S.v.Dubonos, A.A.Firsov, *Nature,* 2005, **438**, 197-200

11.G.Liu, W.Stillman, S.Rumyantsev, Q.Shao, M.Shur, A.A.Balandin, *Appl.Phys.Lett*., 2009, **95**, 0333103

12. M.G.Chung, D.H.Kim, H.M.Lee, T.Kim, J.H.Choi, D.K.Seo, J.-B.Yoo, S.-H.Hong, T.J.Kang, Y.H.Kim, *Sens.Actuators B*., 2012, **166-167**, 172-176

13.X.Li, C.W.Magnuson, A.Venugopal, R.M.Tromp, J.B.Hannon, E.M.Vogel, L.Colombo, and R.S.Ruoff, *J.Am.Chem.Soc.,* 2011, **133**, 2816-2819

14. S.Bhaviripudi, X.Jia, M.S.Dresselhaus, and J.Kong, *Nano Lett.,* 2010, **10**, 4128-4133

15. W.Liu, H.Li, C.Xu, Y.Khatami, K.Banerjee, *Carbon*, 2011, **49**, 4122-4130

16.X.Li, C.W.Magnuson, A.Venugopal, J.An, J.W.Suk, B .Han, M.Borysiak, W.Cai, A.Velarmakanni, Y.Zhu, L.Fu, E.M.Vogel, E.Voelkl, L.Colombo, and R.S.Ruoff, *Nano Lett*., 2010, **10**, 4328-4334

17.G.Lu, L.E.Ocola, and J.Chen, *Appl.Phys.Lett.,* 2009, **94**, 083111

18. N.Yamazoe, G.Sakai, K.Shimanoe, *Catal.Surv.Asia*., 2003, **7(1)**, 63-75

19. J.X.Wang, X.W.Sun, Y.Yang, C.M.L.Wu, *Nanotechnology,* 2009, **20**, 465501

20. A.Rorleo, L.Francioso, S.Capone, P.Sicilano, P.Lomments, Z.Hens, *Sens.Actuators B.,* 2010, **146**, 111-115

21. J.Zhang, S.Wang, Y.Wang, M.Xu, H.Xia, S.Zhang, W.Huang, X.Guo, S.Wu, *Sens.Acutators B*., 2009, **139**, 411-417

22. J.Zhang, S.Wang, Y.Wang, Y.Wang, B.Zhu, H.Xia, X.Guo,S.Zhang, W.Huang, , S.Wu, *Sens.Acutators B*., 2009, **135**, 610-617

23. K.Galatais, L.Cukrov, W.Wlufarski, P.VcCormick, K.Kalantar-Zadeh, E.Comini, G.Sberveglieri, *Sens.Actuators B.,* 2003, **93**, 562-565

24.H.Tang, M.Yan, X.Ma, H.Zhang, M.Wang, D.Yang, *Sens.Actuators B.,* 2006, **113**, 324-328

25.Z.Zhang, R.Zou, G.Song, L.Yu, Z.Chen and J.Hu, *J.Mater.Chem.*, 2011, **21**, 17360-17365

26**.** H.Zhang, J.feng, T.Fei, S.Liu, T.Zhang, *Sens.Actuators B*., 2014, **190**, 472-478

27. H.Mu, Z.Zhang, X.Zhao, F.Liu, K.Wang, and H.Xie, *Appl.Phys.Lett.,* 2014, **105**,033107

28. B.Lee, S.Y.Park, H.-c.Kim, K.Chio, E.M.Vogel, M.J.Kim, R.M.Wallace, and J.Kim, *Appl.Phys.Lett.,* 2008, **92**, 203102

29.Y.Xuan, Y.Q.Wu, T.Shen, M.Qi, M.A.Capano, J.A.Cooper, and P.D.Ye, *Appl.Phys.Lett.*, 2008, **92**, 013101

30. G.Koroteenkov, V.Brinzari, V.Gotovanov, AZ.Cemeavschi, V.Matdin, A.Todd, Acceptor-like Behavior of Reducing Gases on the Surface of n-type In_2O_3, *Appl.Surf.Scie*. **2004**, 227, 122

31. A.K.Prasad, D.J.Kubinski, P.I.Gouma, Comparison of Sol–Gel and Ion Beam Deposited MoO_3 Thin Film Gas Sensors for Selective Ammonia Detection. *Sens.Actuators B.* **2003**, 93, 25-30

32. A.Gurlo, N.Barsan, A.Oprea, MN.Sehm, T.Sahm, U.Weimar, *Appl.Phys.Lett.*, 2004, **85(12)**, 2280-2282

33. H.Yamada, G.R.Miller, *J.Solid State.Chem.,* 1973, **6(1)**, 169-177

34. Z.H.Ni, H.M.Wang, Z.Q.Luo, Y.Y.Wang, T.Yu, Y.H.Wu, Z.X.Shen, *J.Raman.Spectrosc.,* 2010, **41**, 479-483

35.J.T.Robinson, F.K.Perkins, E.S.Snow, Z.We, P.E.Sheehan, *Nano.Lett*., 2008, **8(10)**, 3137-3140

36. C.L.Roy**,** *Czech.J.Phys.B*., 1977**, 27**, 769-776

37. J.Mizsei, *Sens.Actuators B*., 1995, **23**, 173-176

38.N.Hongsith, E.Wongrat, T.Kerdcharoen, S.Choopun, *Sens.Actuators B*.**,** 2010, **144**, 67-72

39.X.Du, S.M.George, *Sens.Actuators B*., 2008, **135**, 152-160

40.J.Xu, Q.Pan,Y. Shun, Z.Tian, *Sens.Actuators B*., 2000, **66**, 277-279

Figure Caption

Fig.1. FESEM Pictures of (a) Pristine graphene, (b) 5 cycles ZnO/graphene, (c) 3nm ZnO/graphene,(d)10nm ZnO/graphene. Inset: The magnified FESEM.

Fig.2 XPS spectra of the 5 cycles and 10nm ALD ZnO films modified graphene, (a) Zn2p, (b) O1s

Fig.3. Raman Spectra of the (a) as-grown graphene (b) pristine graphene (90 seconds ozone treated), (c) 5 cycles ZnO/graphene, (d) 10nm ZnO/graphene.

Fig.4 Temperature dependence of the sensitivity (eye-guided curves) of (a) pristine graphene (90 seconds ozone treated), (b) 5 cycles ZnO/graphene, (c) 1nm ZnO/graphene, (d) 3nm ZnO/graphene, (e) 5nm ZnO/graphene, (f) 10nm ZnO/graphene, upon the exposure to 10 ppm NO_2.

Fig.5 (a) Sensitivity dependence on the ZnO films thickness at various temperature (b) Sensitivity dependence on the NO_2 concentration for the 3nm ZnO/graphene sensors at the operating temperature of 200°C

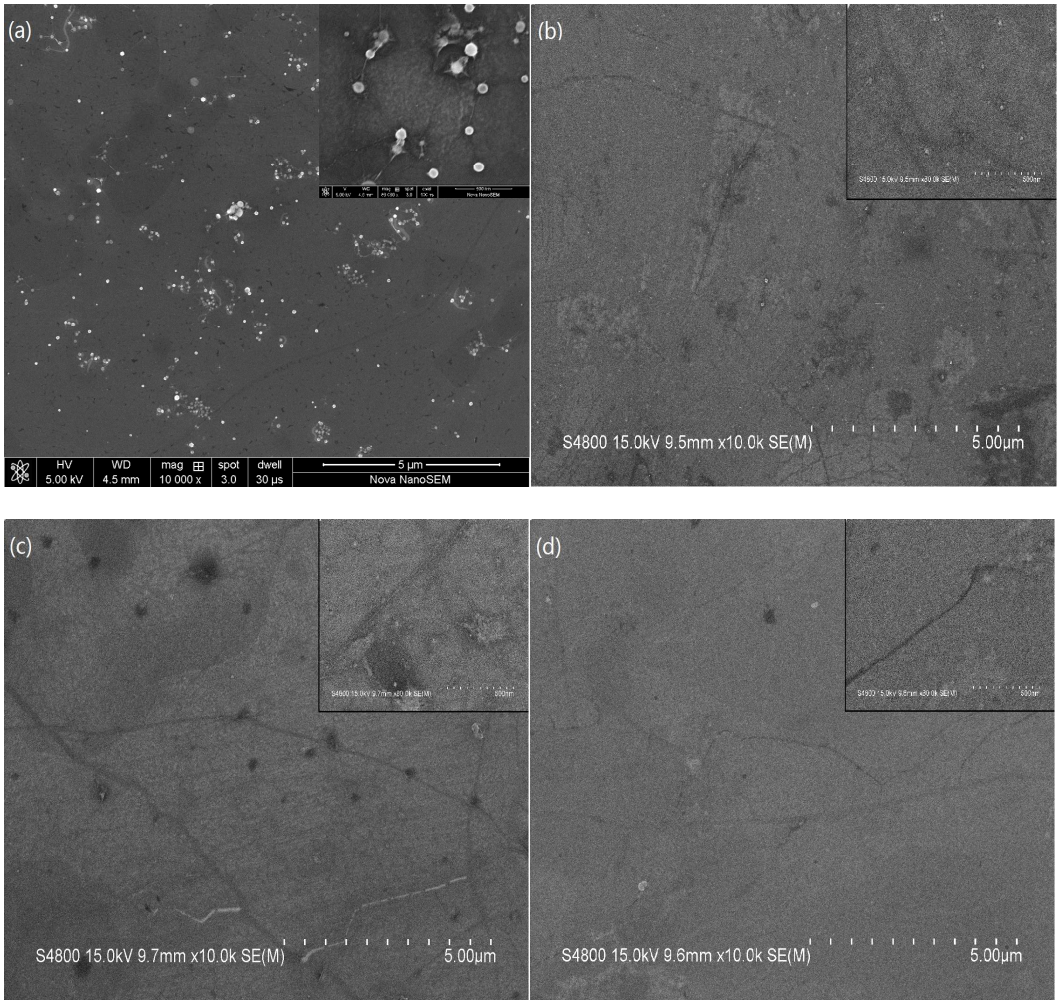

Fig.1

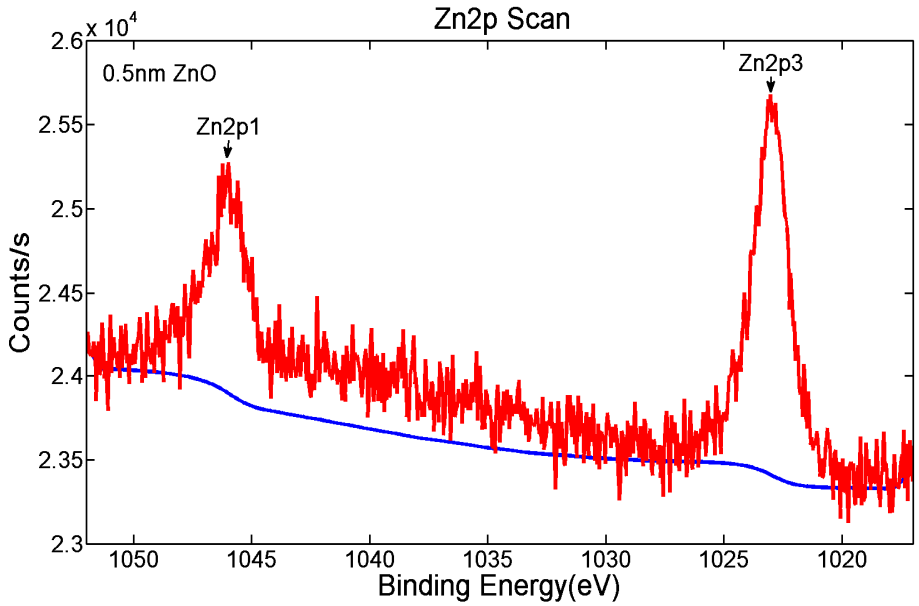

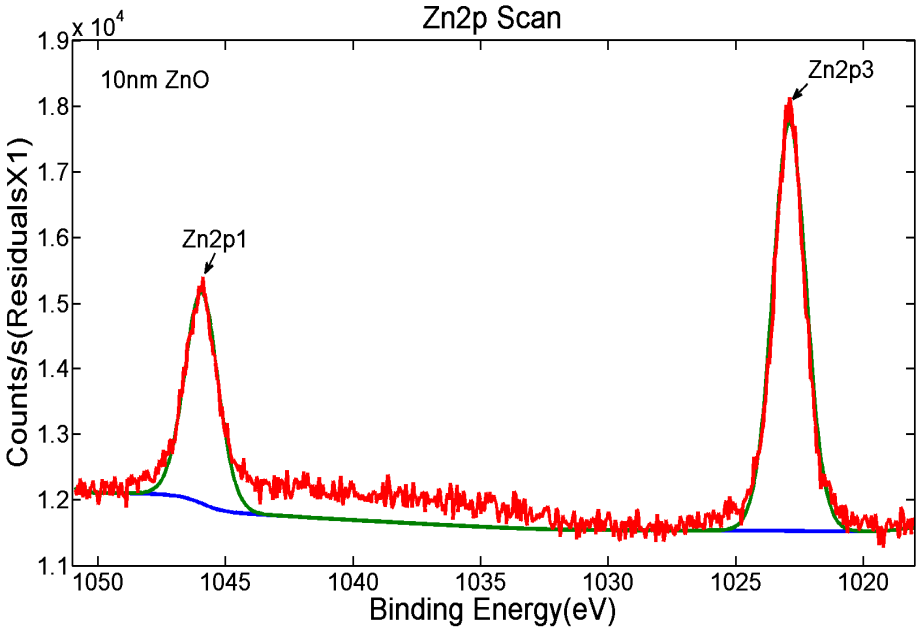

Fig.2(a)

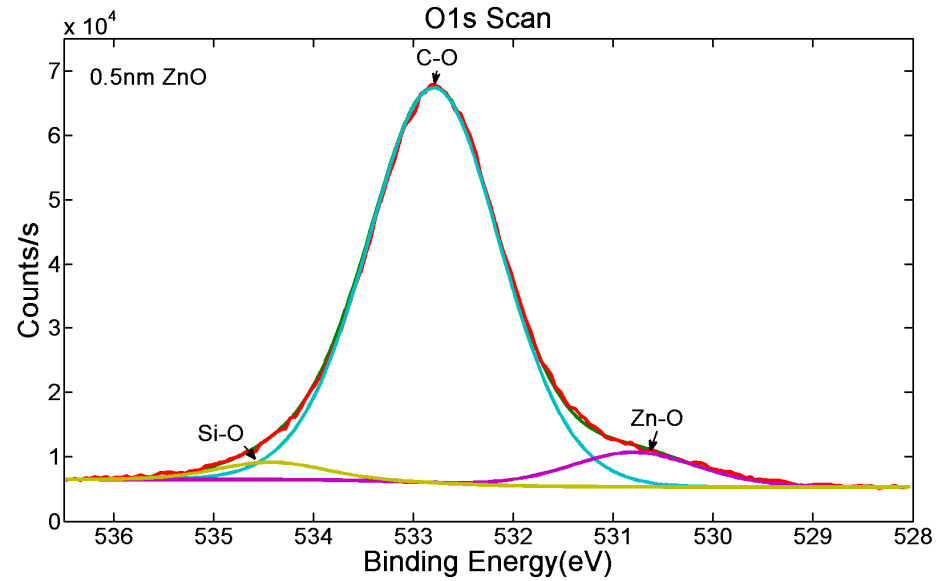

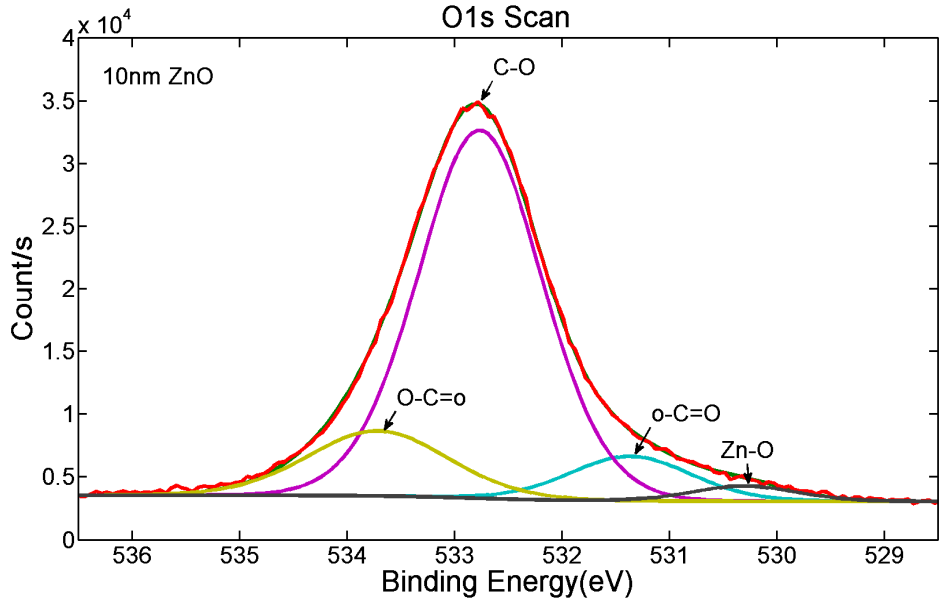

Fig.2(b)

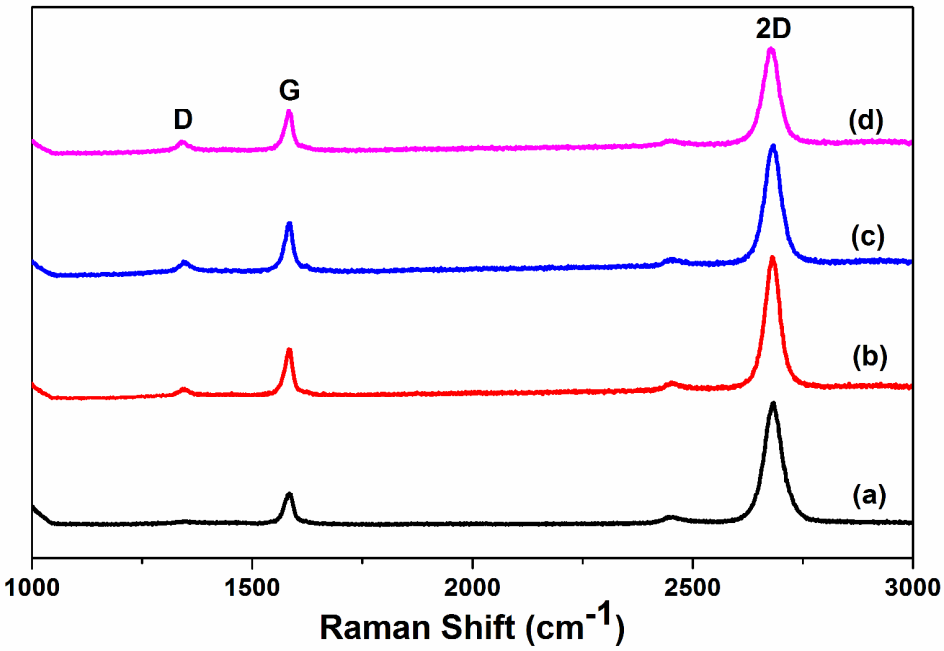

Fig.3

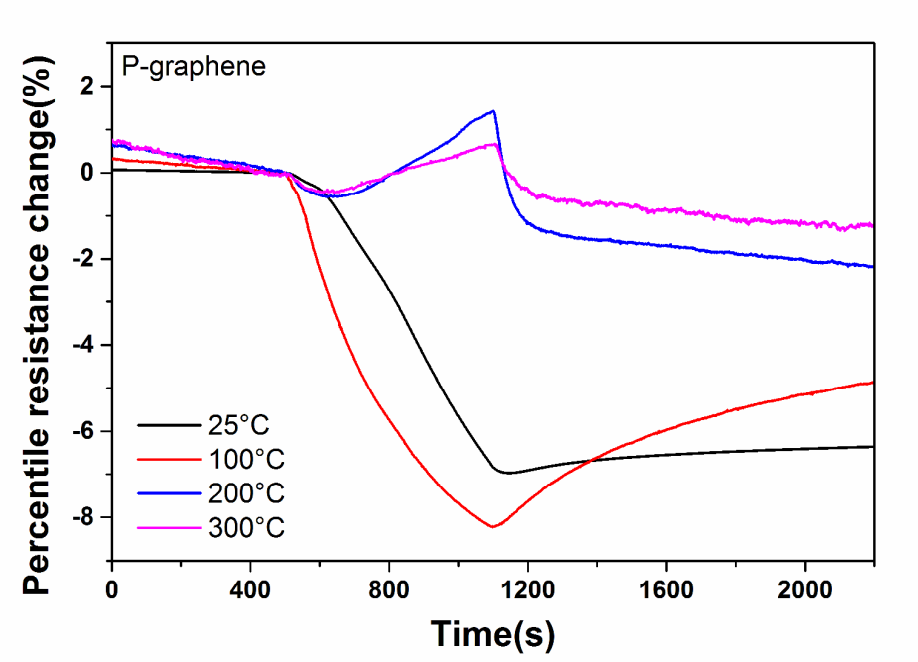

Fig.4(a)

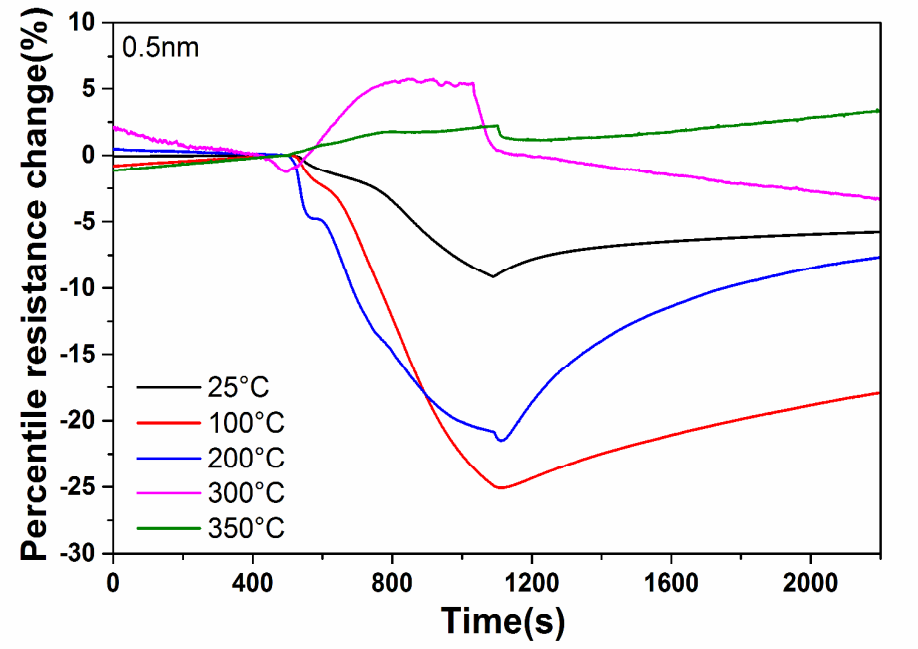

Fig.4(b)

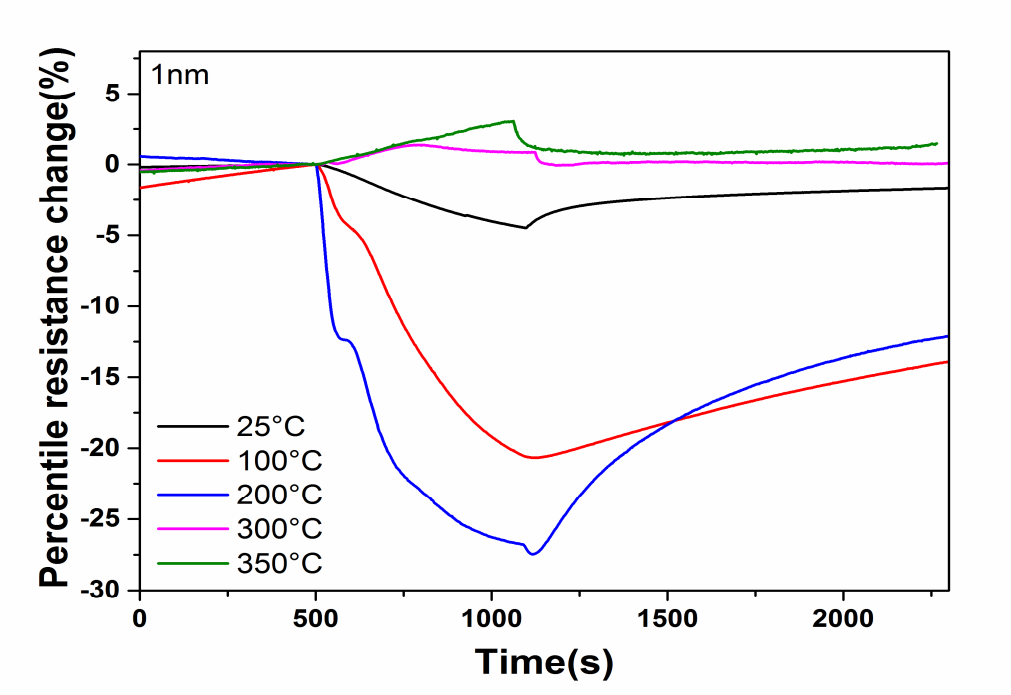

Fig.4(c)

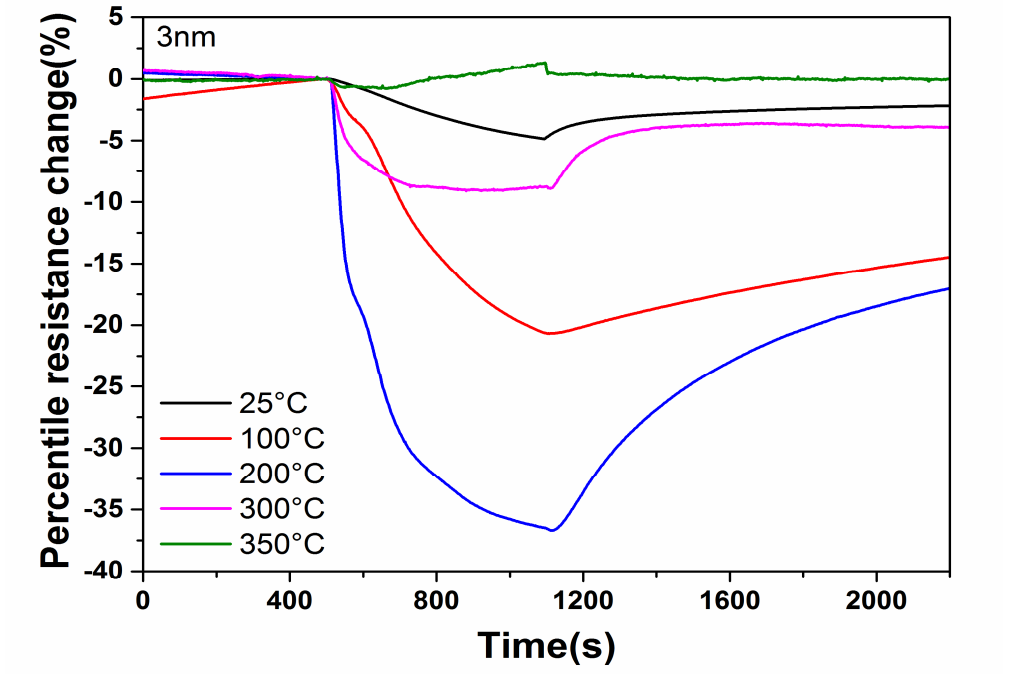

Fig.4(d)

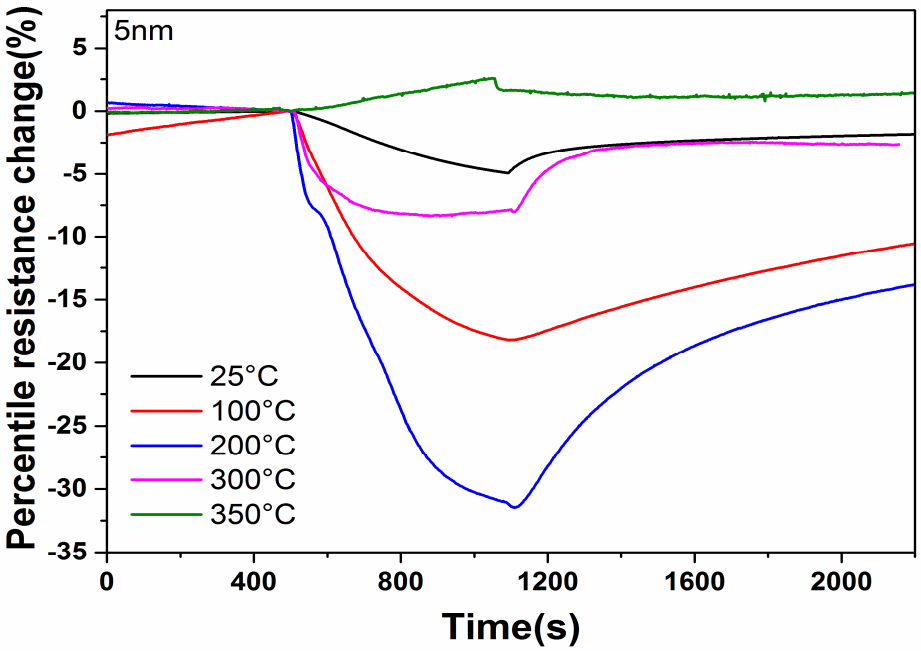

Fig.4(e)

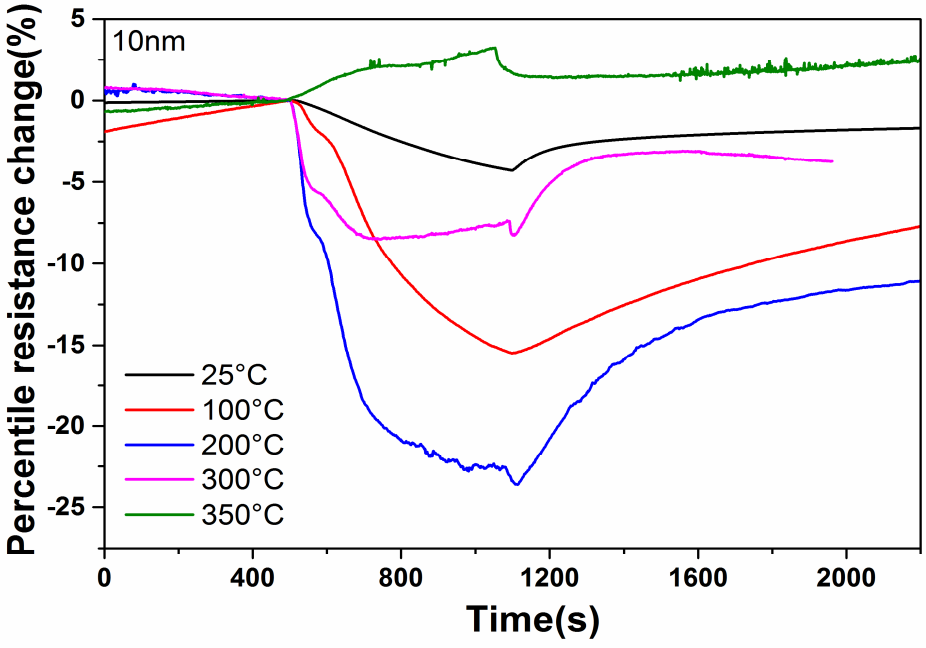

Fig.4(f)

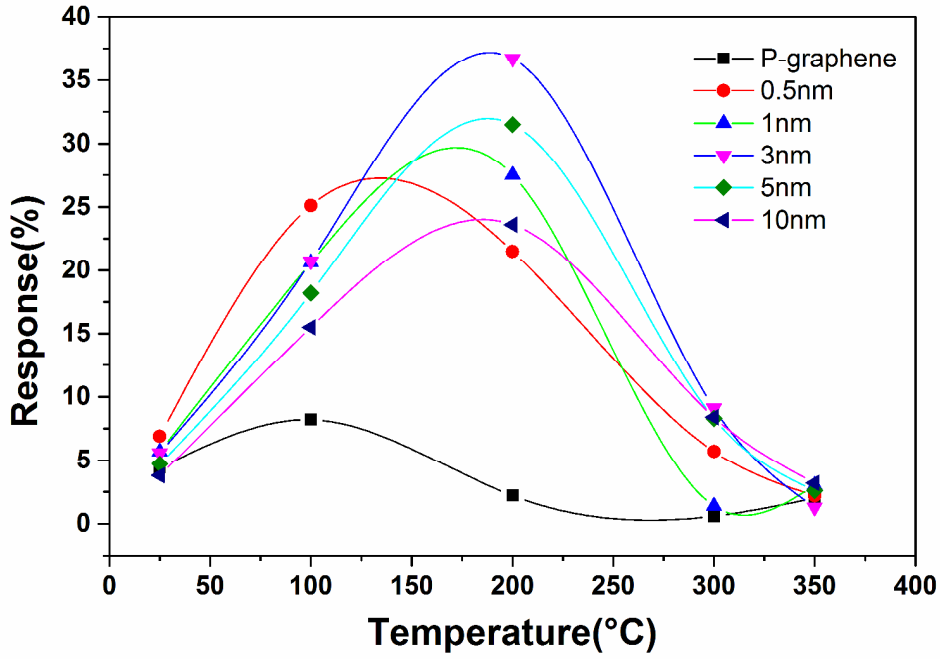

Fig.5(a)

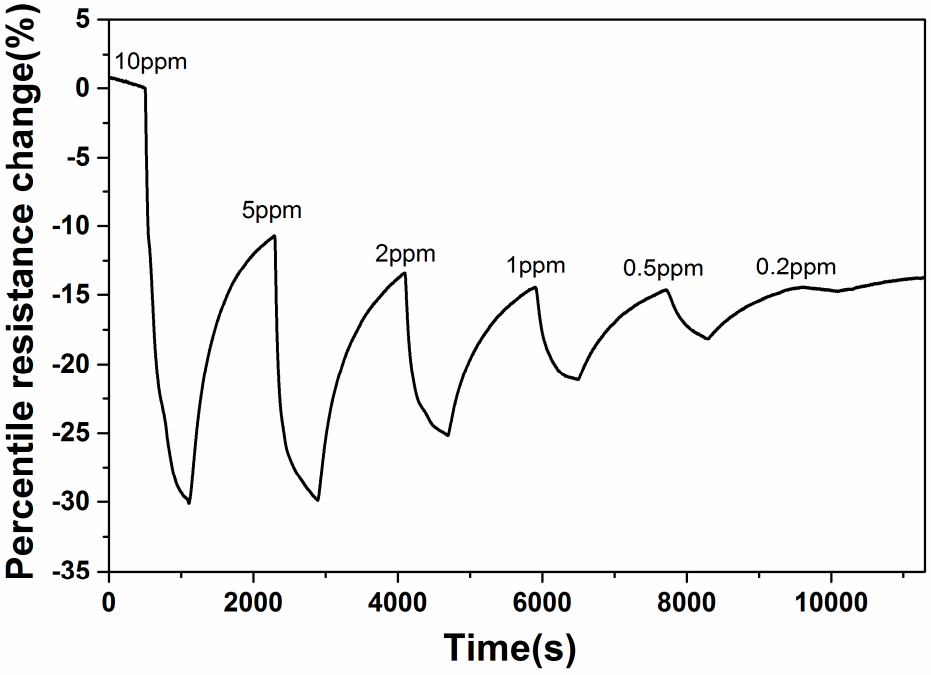

Fig.5(b)

Table 1

Temperature/°C	*25*	*100*	*200*	*300*	*350*
P-graphene	-4.4%	-8.2%	2.2%*	0.6%	2.0%
0.5nm	-6.9%	-25.1%	-21.5%	5.7%*	2.2%
1nm	-5.7%	-20.6%	-27.5%	1.4%*	3.0%
3nm	-5.6%	-20.7%	-36.7%	-9.1%	1.3%*
5nm	-4.7%	-18.2%	-31.5%	-8.3%	2.6%*
10nm	-3.8%	-15.5%	-23.6%	-8.4%	3.2%*

Response of the pristine (P-graphene) and ZnO/graphene sensors with various ZnO films thickness at various operating temperature. Negative response stands for the resistance change (p-type behavior), * represents the p to n conductance transition temperature